Strongly Bonded Bimolecular Complexes between HCN and HNC

Antti Heikkilä*,† and Jan Lundell

Laboratory of Physical Chemistry, P.O. Box 55 (A. I. Virtasen aukio 1), FIN-00014 University of Helsinki, Finland

Received: January 24, 2000; In Final Form: April 12, 2000

The equilibrium structures, vibrational properties, and interaction energies for four bimolecular complexes of HCN and HNC (HCN···HCN, HNC···HNC, HCN···HNC, and HNC···HCN) were studied with ab initio methods. Different electron correlation levels and basis sets up to CCSD(T)/6-311++G(2d,2p) were used in the geometry optimizations and interaction energy calculations, and the vibrational frequencies were calculated at the MP2 and MP3 levels of theory. To study the nature of the intermolecular interactions, an energy decomposition analysis was carried out. For the HNC···HCN complex, which possesses a hydrogen bridge between two carbons, the counterpoise-corrected interaction energy and its decomposition has been calculated as a function of the intermolecular distance. The effect of subunit deformation on the interaction energy has also been considered. The results indicate that the HNC dimer has considerably stronger intermolecular interaction than the HCN dimer, and the HNC···HCN complex is bonded as strongly as the HCN dimer. The comparison of the various properties of the complexes and the energy decomposition analysis in particular indicate that carbon can act as both a hydrogen acceptor and donor, and the resulting hydrogen bonds in these complexes are relatively strong.

Introduction

The participation of carbon in hydrogen bonds is a phenomenon which has recently attracted increased attention as a new, nonclassical form of hydrogen bonding.[1] Particularly, the bonds where carbon is the hydrogen acceptor have been classified as "nonconventional". The first experimental C···H−X bonds in organic isocyanides were reported by Schleyer and Allerhand,[2] and very soon thereafter a C···H−C bond was observed between isonitrile (C_6H_5−NC) and aniline (C_6H_5−NH_2).[3] The strong interaction in these C···H−X type complexes sets them apart from those of carbon π-electron systems,[4,5] and their interaction energies resemble those of the corresponding cyanides.[6]

The simplest comparative study of HNC and HCN as hydrogen bond donors and acceptors would include the $(HCN)_2$ and $(HNC)_2$ dimers and the mixed complexes HCN···HNC and HNC···HCN. The aggregation of HCN has been studied by means of a variety of experimental techniques, and hydrogen bonding has long been recognized as having a profound influence on the properties of HCN through the formation of associated species.[7] The HCN dimer has been already studied extensively both experimentally[8−11] and computationally,[12−14] and all data indicate a linear, hydrogen-bonded complexation between the two HCN monomers.

The other isomer of HCN, hydrogen isocyanide (HNC), was observed for the first time as a UV-photoisomerization product of HCN in low-temperature matrixes[15] and has thereafter been studied in the gas phase as well.[16] HNC has been calculated to be ca. 61 kJ mol^{-1} (5100 cm^{-1}) higher in energy than HCN, and the transition state lies 146 kJ mol^{-1} (12 200 cm^{-1}) above HNC.[17]

The complexes of HNC have been studied to a lesser extent compared to HCN. Ab initio studies on HNC and other isocyanides as hydrogen bond acceptors have been conducted by Alkorta et al.,[18] where the authors considered only complex structures, energetics, and electronic charge densities for various isocyanides as proton acceptors. However, the HCN−HNC complex, where HNC acts as a proton donor, was not included in that study.

Recently, we reported results on both HCN and HNC complexed with water.[19] In that study, two conformers of HCN−H_2O and HNC−H_2O were isolated and identified in low-temperature argon matrix, and extensive ab initio calculations were used to support the interpretation of the experimental results. The complexes were generated as the products of 193 nm photolysis of formaldoxime, and the formation of 1:1 complexes was dependent on the monomericity of the precursor. However, if aggregates of the formaldoxime precursor are present, the $(HCN)_2$, $(HNC)_2$, and HCN−HNC complexes might appear as photoproducts as well. Therefore, the scope of this paper is 2-fold: (i) To study the structural and vibrational properties of the hydrogen-bonded complexes of isocyanic acid $(HNC)_2$, HCN···HNC, and HNC···HCN in order to assist in identifying the possible photoproducts in the ongoing experimental work on the photodecomposition of formaldoxime in various rare gas matrixes; (ii) to study interactions between HCN and HNC in hydrogen-bonded complexes, especially in HNC···HCN containing a C···H−C interaction linkage.

Computational Details

The Gaussian 94 and 98 programs were used for all ab initio calculations.[20,21] All complex structures were optimized considering electron correlation via Møller−Plesset perturbation theory to the second and third order (MP2, MP3). The valence split triple-ζ 6-311G basis set was used with multiple sets of diffuse and polarization functions, i.e., the 6-311++G(d,p) and 6-311++G(2d,2p) basis sets, which have been shown to be reasonably efficient and accurate in reproducing the properties of hydrogen-bonded complexes.[19,22,23]

† E-mail: Antti.Heikkila@csc.fi.

10.1021/jp0002897 CCC: $19.00
Published on Web 06/21/2000

The interaction energies were calculated as the difference of total energy between the complex and the subunits at infinite distance using different electron correlation methods (MP3, MP4, CCSD, CCSD(T)). The interaction energies were corrected for the basis set superposition error (BSSE) by calculating the energy difference between the complex and the monomers in the dimer-centered basis set (DCBS). This corresponds to the counterpoise correction (CP) procedure described by Boys and Bernardi.[24]

An energy decomposition scheme was applied to study the nature of the interactions in the complexes. The complete scheme is based on the Morokuma analysis[25] and its extension to the MP2 level, which has been described previously.[26] In brief, the total interaction energy is decomposed into the SCF (E_{SCF}) and the electron correlation ($E^{(2)}$) contributions. The SCF interaction energy is given as the sum of electrostatic attraction (E_{es}), exchange-repulsion (E_{ex}), and the mutual deformation of the electronic charge clouds (E_{del}^{SCF}), which is called the SCF delocalization term:

$$E_{SCF} = E_{ex} + E_{ex} + E_{del}^{SCF} \quad (1)$$

At distances where intermolecular overlap is small and the intermolecular exchange effects can be neglected, the SCF delocalization term can be approximated by the second-order induction energy with response effects ($E^{20}_{ind,r}$).[27] The sum of E_{es} and E_{ex} is the classical Heitler−London interaction energy ΔE_{HL}.

The correlation contributions to the interaction energy can be decomposed as follows: [28−31]

$$E^{(2)} = E_{disp} + E_{es}^{(12)} + \text{induction correlation} + \text{exchange terms} \quad (2)$$

E_{disp} is the second-order uncoupled Hartree−Fock dispersion energy,[32] and $E_{es}^{(12)}$ is the second-order intrasystem correlation contribution to the electrostatic effect according to ref 26. Only these two energy components have been taken into account in this study, and the two remaining terms, representing the change in the deformation and exchange energies relative to their SCF values, can be regarded as of fairly small magnitude as discussed in the literature.[33] It is important to note that all these energy components are not affected to a priori BSSE since they were calculated in the dimer-centered basis set (DCBS). All interaction energy components were calculated at the MP2/6-311++G(d,p) level of theory.

Results and Discussion

Equilibrium Geometries. The computational equilibrium structures of the $(HCN)_2$, HCN···HNC, HNC···HCN and $(HNC)_2$ complexes are shown in Figure 1, and the structural parameters are collected in Table 1. As has been shown computationally[8−11] and experimentally[12−14] the HCN dimer is a linear hydrogen-bonded complex, and therefore, all complexes presented here have been constrained in the $C_{\infty v}$ point group.

The HCN dimer is the only one of the complexes presented in this work for which an experimental structure derived from microwave experiments exists.[9] Generally, a reasonable agreement between the calculated and experimental structures is noted. In the proton acceptor HCN the experimentally determined values are 1.0634 Å for the C−H bond and 1.1226 for the C−N bond, and the corresponding values for the proton donor are 1.2463 Å for the C−H bond and 1.1399 Å for the C−N bond.

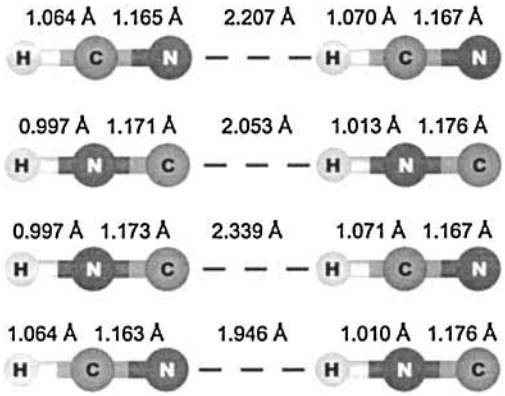

Figure 1. The calculated (MP2/6-311++G(2d,2p)) linear structures of $(HCN)_2$, $(HNC)_2$, HNC···HCN, and HCN···HNC. Distances are given in Å.

Our calculations at the MP2/6-311++G(2d,2p) level give values of 1.064 Å for the C−H and 1.165 Å for the C−N bond of the proton acceptor, which are close to the experimental results. The calculated values of proton donor bond lengths are 1.070 and 1.17 Å for the C−H and C−N bonds, respectively. The calculated donor C−H bond length is 0.18 Å smaller than the experimentally determined value, whereas the calculated and experimental values for the C−N bond are very close to each other. An explanation for the discrepancy between the experimental and calculated donor C−H bond values is the short distance (0.4 Å) between the donor hydrogen and the center of mass of the complex, which decreases the accuracy of the experimental bond length, as indicated in the analysis of the MW spectra by Ruoff et al.[9]

The experimental intermolecular distance was 2.265 Å from the proton donor hydrogen to the proton acceptor nitrogen. At the MP2/6-311++G(d,p) level this is exactly the one found computationally, but the addition of polarization functions to the basis set shortens the intermolecular bond distance to 2.207 Å.

The structures of the other complexes reflect the HCN dimer. Upon complexation the proton donor bonds are elongated compared to the unperturbed monomers whereas the proton acceptor bonds appear to be less sensitive for the interaction. Comparing the intermolecular distances at the MP2/6-311++G(2d,2p) level of theory indicates that all four complexes studied represent relatively strong hydrogen-bonded complexes. The calculated intermolecular distances sets the complexes in the following order: HCN···HNC < $(HNC)_2$ < $(HCN)_2$ < HNC···HCN. It must be noted here that these four complexes formed from HCN and HNC show four different hydrogen bonds upon complexation. The two shortest interactions, i.e., N···H−N (1.946 Å) and C···H−N (2.053 Å), involve a N−H proton donor group which is generally regarded as a good hydrogen-bond former.[34] Additionally, in both of these complexes HNC acts as a proton donor. The two longest intermolecular distances are found for the complexes where HCN acts as proton donor indicating that HCN forms weaker complexes than HNC. It is well-known that HCN is a good proton acceptor but a much weaker proton donor.[18,34] This is mainly due to the weak proton donor abilities of the C−H group, which is now acknowledged to be able to form hydrogen bonds.[35] However, unlike most C−H bonds which are poor proton donors, the triple bond to the carbon atom makes HCN a rather effective proton donor. In the $(HCN)_2$ dimer the CH group interacts with the nitrogen atom of the proton acceptor. When the HCN acceptor is replaced by HNC, the interaction occurs via a hydrogen bridge

TABLE 1: Geometrical Parameters[a] of the Linear $(HCN)_2$, $(HNC)_2$, and HCN−HNC Complexes at the MP2/6-311++G(d,p), MP2/6-311++G(2d,2p), and MP3/6-311++G(2d,2p), Levels

	$(HCN)_2$			$(HCN)_2$			HCN···HNC			HCN···HNC		
	(d,p)	(2d,2p)	MP3	(d,p)	(2d,2p)	MP3	(d,p)	(2d,2p)	MP3	(d,p)	(2d,2p)	MP3
$r(CH_a)$	1.069	1.064	1.063				1.069	1.064	1.063			
$r(NH_a)$				1.002	0.997	0.993				1.002	0.997	0.993
$r(CN_a)$	1.170	1.165	1.145	1.170	1.171	1.158	1.169	1.163	1.144	1.179	1.173	1.160
$r(CH_d)$	1.074	1.070	1.068							1.074	1.071	1.069
$r(NH_d)$				1.016	1.013	1.005	1.013	1.010	1.003			
$r(CN_d)$	1.171	1.167	1.147	1.181	1.176	1.162	1.181	1.176	1.162	1.172	1.167	1.147
r(interaction)	2.265	2.207	2.233	2.091	2.053	2.109	1.983	1.946	1.991	2.407	2.339	2.372

[a] Bond distances are given in Å The subscript d refers to the hydrogen bond donor, and a refers to the acceptor.

TABLE 2: Geometrical Parameters[a] of the HNC···HCN Complex[a]

	MP2/6-311++G(d,p)		MP2/6-311++G(2d,2p)		MP3/6-311++G(2d,2p)	CCSD(T)/6-311++G(2d,2p)
	$C_{\infty v}$	C_s	$C_{\infty v}$	C_s	$C_{\infty v}$	C_s
r(NH)	1.002	1.0016	0.997	0.9968	0.9926	0.9973
$r(CN_1)$	1.1788	1.1788	1.173	1.1731	1.1601	1.1723
r(CH)	1.0744	1.0745	1.071	1.0708	1.0687	1.0734
$r(CN_2)$	1.1719	1.172	1.167	1.1670	1.1470	1.1606
r(interaction)	2.4074	2.4015	2.339	2.3377	2.3721	2.3647
∠(HNC)	180.00	179.95	180.00	179.94	180.00	179.99
∠(NC···H)	180.00	179.59	180.00	179.71	180.00	179.96
∠(C···HC)	180.00	179.78	180.00	179.67	180.00	179.97
∠(HCN)	180.00	180.01	180.00	180.05	180.00	180.00
r(NH, HNC monomer)	1.0005		0.9958		0.9916	0.9962
r(CN, HNC monomer)	1.1816		1.1761		1.1635	1.1757
r(CH, HCN monomer)	1.0680		1.0633		1.062	1.0664
r(CN, HCN monomer)	1.1714		1.1665		1.1465	1.1601

[a] Bond distances are given in Å and bond angles, in deg. $r(CN_1)$ is the CN bond length of HNC, and $r(CN_2)$, the CN bond length of HCN.

between two carbon atoms. This prompted us to study the C−H···C interaction in more detail.

The HNC−HCN complex structure was optimized both constraining the complex into a linear configuration and in the C_s symmetry at the MP2/6-311++G(d,p) and MP2/6-311++G(2d,2p) levels. Additionally, the equilibrium structure was studied at the MP3 and CCSD(T) levels using the larger basis set. The results are collected in Table 2 along with the MP2 results and compared with the monomer values. All calculations indicate that the HNC−HCN complex is linear. The intermolecular distance between the CH group hydrogen and the proton acceptor carbon decreases when the number of polarization functions is increased. On the contrary, the intermolecular C−H···C distance is increased by 0.0344 Å by the substitution of MP3 for MP2. The improved electron correlation of CCSD(T) decreases the intermolecular distance compared to the MP3 level, and the CCSD(T) calculated value of 2.3647 Å is between the MP2 and MP3 values. At all levels the donor C−H bond distance is found to increase by ca. 0.007 Å, while the other bonds change ca. 0.001−0.003 Å compared to the monomer values. Generally, the MP2 and CCSD(T) levels give similar results indicating that the MP2 picture is already reasonably good.

Interaction Energies. The interaction energies in the supermolecular Møller−Plesset perturbation theory (MPPT) and its infinite-order coupled cluster (CC) generalizations are presented in Table 3. The MP2/6-311++G(2d,2p) optimized structures for all complexes were used. The interaction energies were obtained as the difference between the energy of the complex and the sum of energies of the subunits in the dimer-centered basis set (DCBS):

$$E_{int} = E_{AB} - (E_A + E_B) \tag{3}$$

In this approach the interaction energies are corrected for the BSSE, but the subunits are considered in the complex geometries. Recently, van Duijnevelt [36] proposed a new scheme for calculating the interaction energy where deformation of the subunits upon complexation is taken into account:

$$E_{int} = E_{AB} - [(E_A + E_A^{def}) + (E_B + E_B^{def})] \tag{4}$$

TABLE 3: BSSE-Corrected Interaction Energies and Deformation Energies of the $(HCN)_2$, $(HNC)_2$, HCN···HNC, and HNC···HCN Complexes[a]

	$(HCN)_2$	$(HNC)_2$	HCN···HNC	HNC···HCN
Interaction Energies E_{int} (kJ mol^{-1})				
MP2//MP2	−17.746	−29.495	−28.406	−18.101
MP3//MP2	−16.747	−25.025	−24.659	−16.359
MP4SDQ//MP2	−16.958	−25.371	−25.144	−16.466
CCSD//MP2	−16.641	−24.630	−24.439	−15.780
CCSD(T)//MP2	−16.826	−25.983	−25.175	−16.278
MP3//MP3	−17.854	−27.579	−27.036	−17.855
MP4SDQ//MP3	−17.789	−27.707	−27.242	−17.804
CCSD//MP3	−17.594	−27.082	−26.751	−17.216
CCSD(T)//MP3	−17.947	−28.566	−27.650	−17.898
CCSD(T)				−17.676
CCSD(T) + E^{def}				−17.523
Deformation Energies E^{def} (kJ mol^{-1})				
MP2	0.092	0.792	0.505	0.154
MP3	0.084	0.613	0.386	0.153
CCSD(T)				0.153

[a] The 6-311++G(2d,2p) basis set has been used in all calculations.

These deformation (E^{def}) energies are also shown in Table 3 for the various complexes. As can be seen, the deformation energies are very small compared to the total interaction energies and the values calculated at the MP2, MP3 and CCSD(T) levels for the HNC···HCN complex are the same. For all complexes, the deformation energy corrections to the total interaction energy are nominal, and the interaction energies calculated in the DCBS approach should be considered accurate enough.

The BSSE-corrected interaction energies for the studied complexes indicate moderately strongly bound complexes,

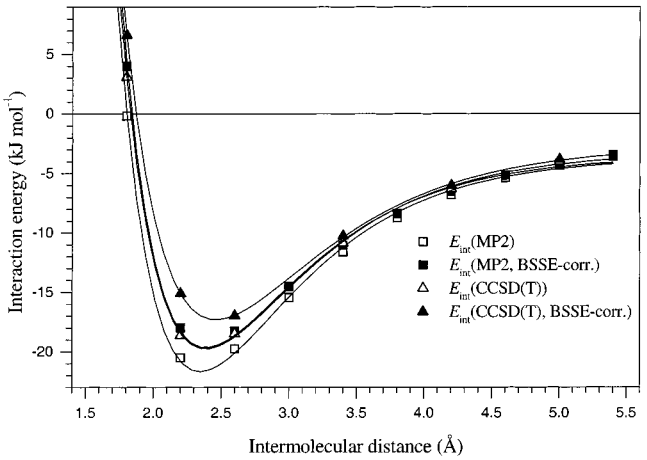

Figure 2. Plot of the interaction energy, E_{int} (in kJ mol^{-1}), of HNC···HCN as a function of the interaction distance in Å. The internal coordinates of the subunits are fixed to their values in the equilibrium geometry of the complex (see Table 2). See text for details.

which is in agreement with the relatively short intermolecular distances found for these complexes. The HNC dimer is the most strongly bonded complex, and HCN···HNC has a fairly similar interaction energy, ca. −25 kJ mol^{-1} at the CCSD(T)//MP2 level. The interaction energies of the complexes where HCN acts as a proton donor, i.e. $(HCN)_2$ and HNC···HCN, are close to ca. −15 kJ mol^{-1}. These similarities are readily explained by the HNC hydrogen donor common to HNC dimer and HCN···HNC and the HCN hydrogen donor common to HCN dimer and HNC···HCN. Also in the study of Alkorta et al.[18] HNC was found to be a better hydrogen donor than HCN.

At the MP2 level, the HNC···HCN complex is slightly more tightly bound than $(HCN)_2$. At the CCSD(T)//MP2 level the order is reversed. However, the differences are small at all levels of theory. When the HNC···HCN complex structure is optimized at the CCSD(T)/6-311++G(2d,2p) level, the calculated interaction energy increases by ca. 1 kJ mol^{-1} from the MP2 value. This indicates that the increased electron correlation does not deform the complex structure from the MP2 calculated one, as was noted from the inter- and intramolecular geometrical parameters shown in Table 2. This can be seen in Figure 2 as well, where the BSSE-contaminated and BSSE-corrected interaction energies are plotted as a function of the HNC···HCN intermolecular distance. The BSSE-contaminated intermolecular potentials show a deeper minimum compared to the BSSE-corrected one. Even though the evaluation of BSSE itself could be considered meaningless after applying the counterpoise correction method in the context of interaction energy,[37] it is interesting to note that the BSSE-corrected intermolecular potential for the HNC···HCN interaction is very close to the BSSE-uncorrected potential calculated at the CCSD(T) level. However, the BSSE-corrected intermolecular potential at the CCSD(T) is slightly less attractive than the MP2 one.

The DCBS-calculated interaction energy components are collected in Table 4. For a typical hydrogen-bonded complex the E_{es} and E_{ex} components represent the largest contributions to the interaction energy, and the SCF deformation energy is similar to the classical Heitler−London interaction energy. For the complexes studied here the electrostatic attraction and exchange repulsion are the largest components, but for all four complexes attractive Heitler−London interaction energies are found. The largest electrostatic interactions are found for $(HNC)_2$ (−38.26 kJ mol^{-1}) and HCN···HNC (−37.58 kJ mol^{-1}), highlighting the favorable linear arrangement of the dipole

TABLE 4: Components of Interaction Energies Calculated in the Dimer-Centered Basis Set (DCBS)[a]

	HCN···HCN	HNC···HNC	HC···HNC	HNC···HCN
E_{es}	−25.49	−38.26	−37.58	−23.87
E_{ex}	13.53	34.36	28.25	15.73
ΔE_{HL}	−11.96	−3.90	−9.33	−8.14
E_{SCF}	−17.66	−18.89	−22.44	−14.12
ΔE_{del}^{SCF}	−5.70	−14.99	−13.11	−5.98
$E^{(2)}$	−0.06	−10.70	−6.23	−3.98
E_{disp}	−5.50	−9.26	−9.03	−5.20
$E_{es}^{(12)}$	5.43	−1.44	2.80	1.22
E_{int}	−17.72	−29.59	−28.67	−18.10

[a] All values have been calculated at the MP2/6-311++G(d,p) level and are given in kJ mol^{-1}.

moments[38] of both subunits as well as strong overlap between wave functions of both subunits. This is the reason for the large SCF delocalization energies for the HNC proton donor complexes as well.

The dispersion energy, E_{disp}, represents the most important contribution among the correlation terms. The largest dispersion energy contributions are found for the HNC proton donor complexes being ca. −9 kJ mol^{-1}. For the HCN proton donor complexes the dispersion energy contributions are smaller being around −5 kJ mol^{-1}. Typically the remaining correlation terms are repulsive in nature, so that the MP2 interaction energy is much less negative than the dispersion component.[26] This is true for all other studied complexes except the $(HNC)_2$ dimer, where the $E_{es}^{(12)}$ component is estimated to be −1.44 kJ mol^{-1}. This is due to the neglected induction correlation and exchange terms when decomposing the electron correlation only to dispersion and second-order electrostatic correlation energy, which might play a more significant role in this complex. Due to the large SCF delocalization energy in the SCF interaction energy also the second-order deformation correlation correction to the SCF deformation should play a more important role for this complex. For all the other three complexes the SCF delocalization energies are smaller than for the $(HNC)_2$ dimer and the net effects of the correlation terms, excluding the dispersion energy, are slightly positive, i.e., repulsive in nature.

It is interesting that the electron correlation terms do not increase the interaction for the $(HCN)_2$ dimer compared to the Hartree−Fock level. The net effect of electron correlation is only −0.06 kJ mol^{-1}, and generally the entire interaction is accounted for at the SCF level. For the other HCN proton donor complex HNC···HCN ca. 22% of the interaction comes from the electron correlation which is similar to the mixed HCN···HNC complex as well (22%). For the $(HNC)_2$ dimer this ratio is 36%, indicating that the electron correlation is much more important when HNC subunit is involved in the complexation. The HCN electron structure is well described already at the SCF level whereas HNC requires electron correlation to be included to be properly described.

One of the most intriguing questions about hydrogen-bonded complexes is "why is a hydrogen bond formed?" This is especially an interesting question when a C−H···C interaction is of concern. To obtain more insight into the nature of this hydrogen-bonded interaction, the energy decomposition components were studied as a function of the intermolecular distance keeping all intramolecular bonds frozen. These energy components are plotted in Figure 3. The major part of the HNC···HCN interaction is obtained at the SCF level, which is typical for interaction between polar systems.[26] The dominant attractive contribution to the binding energy is the electrostatic interaction, which appears to be the interaction component responsible for

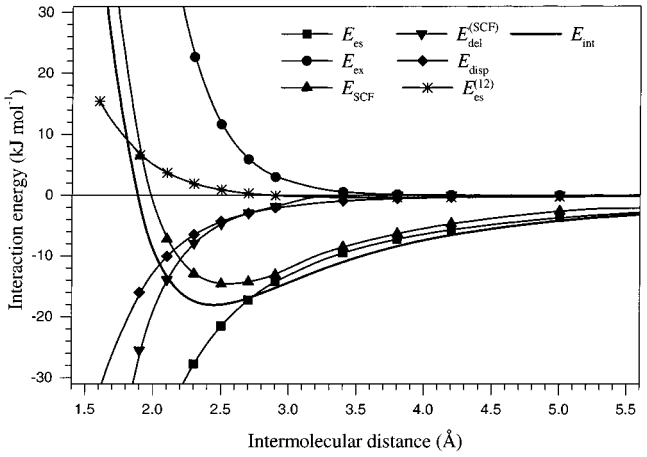

Figure 3. Plot of the interaction energy components (in kJ mol^{-1}) of HNC···HCN as a function of the interaction distance r_{int}. The interaction energy energy components are calculated at the MP2/6-311++G(d,p) level of theory.

the attraction beyond 3.5 Å. The other important contribution, E_{ex}, rapidly grows as the intermolecular distance diminishes. Introducing the repulsive exchange interaction creates a minimum in the Heitler−London interaction energy, which is shifted to shorter distances when the SCF delocalization energy is taken into account. In fact, both ΔE_{HL} and E_{del}^{SCF} are crucial for the production of more-tightly bound complexes. The dispersion energy is heavily distance dependent and dies off quite rapidly like the SCF delocalization and exchange energies. The dispersion energy appears also as reciprocal to the exchange energy indicating that a large dispersion contribution corresponds to a large exchange interaction, which is what we have found in all four complexes and not just in the CH···C interaction. All in all, the total interaction energy of the C−H···C interaction is a result of a delicate balance between all components of the interaction energy, and the energy decomposition analysis convincingly shows that the C−H···C is similar to more conventional hydrogen-bonded interactions.

Vibrational Frequencies. The harmonic vibrational frequencies of the bimolecular complexes of HCN and HNC were calculated at the MP2/6-311++G(2d,2p) and MP3/6-311++G-(2d,2p) levels, and they are compared with monomer frequencies in Table 5.

$(HCN)_2$. For the HCN dimer the largest shifts are found for the CH stretching mode of the hydrogen bond donor and the HCN bending mode of the acceptor. The CH stretch is red-shifted by 50 and 70 cm^{-1}, and the HCN bending mode undergoes a blue shift of 107 and 122 cm^{-1}, calculated at the MP2 and MP3 levels. Experimentally, the hydrogen-bonded CH stretch has been observed in the gas phase[39,40] and in low-temperature Ar matrix.[41] In the gas phase the mode is shifted ca. −70 cm^{-1} and in solid Ar ca. −100 cm^{-1} from the monomer value, both values being in close agreement with the calculated shifts in this work. Similarly, the calculated shifts of the HCN bending mode are close to the value found in an Ar matrix (+77 cm^{-1}).

The other modes of the HCN dimer shift to a lesser extent, and the frequency shifts are accompanied by enhancements of absorption intensity changes typical of hydrogen-bonded complexes. In the gas-phase experiments, the two CN modes are found at 2105 and 2095 cm^{-1}, being shifted +12 and −2 cm^{-1} from the monomer value.[40] In solid Ar the shifts are slightly larger, +24 and +3, respectively, which are qualitatively similar to the calculated shifts.

An interesting phenomenon is observed with the CH stretch not participating in the hydrogen bond: at the MP2 level the mode is estimated to be blue shifted by 19.3 cm^{-1}, whereas at the MP3 level the mode is predicted to be red shifted by 4.7 cm^{-1}. Experimental evidence from low-temperature matrixes indicate that the MP3 calculations are closer since a red shift of 2 cm^{-1} was found in solid Ar.[41] A similar but less dramatic effect is observed also for the CN stretch of the proton acceptor. It seems that the MP3 calculations provide an increased overall reliability for vibrational shift estimations compared to the MP2 calculations. This has already been pointed out in the cases of $(H_2O)_2$,[42] $(HF)_2$, and $(HCl)_2$.[43]

HCN···HNC. This is the other complex where hydrogen cyanide is involved, now as an proton acceptor. The complex is slightly weaker than the $(HCN)_2$ dimer, but still large shifts can be expected for the modes involved in the hydrogen bonding. The largest changes in the vibrational frequencies are found for the NH stretch and HNC bend of the HNC subunit. The NH stretch is predicted to shift strongly to the red, ca. 200−240 cm^{-1} depending on the computational level. Even a stronger shift, about 300 cm^{-1} to the blue, is found for the HNC bend. Both of these shifts are in accord with the previous results for HNC acting as a proton donor.[18,19] The CN acceptor unit on HCN is less perturbed upon complexation, and the predicted shifts are ca. 25−30 cm^{-1} compared with the unperturbed monomer.

The MP2 and MP3 calculations give quite similar results in general for the intermolecular modes of the HCN···HNC complex. However, as noted already for the $(HCN)_2$ dimer, the vibrational shift of the CN stretch is highly dependent on the correlation treatment used in the calculations. At the MP2 level a few wavenumbers red shift of ν_{CN} is found, whereas the MP3 calculation predicts a blue shift of + 6.8 cm^{-1} for this mode. Clearly, the improvement in electron correlation affects mostly the HNC subunit, especially the nonbonding electrons localized on the CN bond.

$(HNC)_2$. This is the most strongly bound complex among the ones studied here, and large perturbations in the vibrational properties of the subunits are expected. The most affected modes upon complexation are the NH stretch and HNC bend of the proton donor subunit. The NH stretch is red shifted by ca. 250 cm^{-1}, and the HNC bend is blue shifted over 300 cm^{-1} from the monomer band positions; this should make experimental identification of this complex quite straightforward. The vibrational modes of the other HNC subunit acting as a proton acceptor are less profound and follow the pattern set by HCN···HNC and $(HCN)_2$.

HNC···HCN. This is the other complex where HCN acts as a proton donor and is of equal strength with the $(HCN)_2$ dimer. In the HNC···HCN complex the degeneracy of the HNC bending mode is broken at the MP3 level even though the complex is linear, but this is probably due to a relatively flat potential energy surface and numerical derivation of force constants. However, the frequencies of the HNC bending modes are close to each other, separated by ca. 6 cm^{-1}, and at the MP2 level the bending modes for both subunits in the complex are degenerate.

The largest shifts of the vibrational frequencies are found for the CN stretch of the proton donor HCN and the bending mode of the proton acceptor HNC. The CH stretch is predicted to shift −65 and −88 cm^{-1} at the MP2 and MP3 levels, respectively. For the HCN bend the shift is ca. +120 and +140 cm^{-1} at the MP2 and MP3 levels, respectively. For the HNC bend the shift is smaller, ca. +20 cm^{-1}. In general, the

TABLE 5: MP2/6-311++G(2d,2p) and MP3/6-311++G(2d,2p) Vibrational Frequencies of the $(HCN)_2$, $(HNC)_2$, and HCN−HNC Complexes

	MP2			MP3		
assgnt	ω (cm^{-1})	I ($kmmol^{-1}$)	$\Delta\omega$ (cm^{-1})	ω (cm^{-1})	I ($kmmol^{-1}$)	$\Delta\omega$ (cm^{-1})
			$(HCN)_2$			
ν_1. $\nu_{non-bonded}$(CH)	3340.3	81.4	19.3	3344.7	67.9	−4.7
ν_2. $\nu_{H-bonded}$(CH)	3271.4	332.7	−49.6	3278.7	324.3	−70.7
ν_3. $\nu_{H-bonded}$(CN)	1950.1	13.9	15.9	2163.8	10.3	16.0
ν_4. $\nu_{non-bonded}$(CN)	1934.3	5.8	0.1	2141.6	20.3	−6.2
ν_5. $\delta_{H-bonded}$(HCN)	796.9	50.3	107.0	845.0	79	122.2
ν_6. $\delta_{non-bonded}$(HCN)	706.7	36.3	16.9	732.0	72.4	9.2
ν_7. δ_{as}(intermolecular)	131.1	44.4		146.4	95.2	
ν_8. ν(intermolecular)	107.1	0.06		112.9	1.8	
ν_9. δ_s(intermolecular)	42.2	7.8		51.4	12.8	
			HCN···HNC			
ν_1, ν(NH)	3429.6	1173.5	−238.8	3527.7	1116.3	−202.5
ν_2, ν(CH)	3319.7	137.1	−1.3	3344.2	110.7	−5.26
ν_3, $\nu_{H-bonded}$(CN)	1962.9	0.9	28.6	2172.4	7.3	24.7
ν_4, $\nu_{non-bonded}$(CN)	1929.2	1.3	−2.9	2069.7	18.6	6.8
ν_5, δ(HNC)	716.4	138.5	288.7	705.3	284.8	279.6
ν_6, δ(HCN)	702.3	27.9	12.5	738.2	62.8	15.4
ν_7, δ_{as} (intermolecular)	156.7	5.2		148.9	4.3	
ν_8, ν(intermolecular)	147.0	24.2		147.3	48.0	
ν_9, δ_s(intermolecular)	61.1	4.6		63.9	11.0	
			$(HNC)_2$			
ν_1, $\nu_{non-bonded}$(NH)	3671.9	293.8	3.5	3710.2	301.3	−20.0
ν_2, $\nu_{H-bonded}$(NH)	3415.3	1305.5	−253.1	3486.0	8.8	−244.3
ν_3, $\nu_{H-bonded}$(CN)	1972.4	20.0	40.3	2105.4	19.8	42.5
ν_4, $\nu_{non-bonded}$(CN)	1931.4	0.09	−0.7	2065.9	17.7	3.0
ν_5, $\delta_{H-bonded}$(HNC)	763.7	142.9	336.1	728.9	255.4	303.2
ν_6, $\delta_{non-bonded}$(HNC)	527.4	142.4	99.8	467.1	276.0	41.4
ν_7, δ_{as} (intermolecular)	169.0	27.7		162.0	45.8	
ν_8, ν(intermolecular)	136.8	4.1		141.8	3.2	
ν_9, δ_s(intermolecular)	72.2	3.0		74.2	3.6	
			HNC···HCN			
ν_1, ν(NH)	3675.7	307.0	7.3	3716.5	327.6	−13.7
ν_2, ν(CH)	3255.8	340.2	−65.2	3260.9	314.9	−88.5
ν_3, $\nu_{H-bonded}$(CN)	1954.1	21.6	22.0	2088.3	69.4	25.4
ν_4, $\nu_{non-bonded}$(CN)	1931.3	10.9	−2.9	2140.2	17.4	−7.6
ν_5, δ(HCN)	808.4	45.6	118.5	859.8	74.5	137.0
ν_6, δ(HNC)	513.7	148.6	86.1	452.2	138.1	26.4
				446.2	140.8	20.5
ν_7, δ_{as}(intermolecular)	146.4	48.2		168.3	48.9	
				163.8	49.1	
ν_8, ν(intermolecular)	101.0	1.2		106.8	1.3	
ν_9, δ_s(intermolecular)	53.6	5.9		85.5	0.9	
				63.1	3.5	

vibrational modes of the complex subunits are perturbed similarly to the $(HCN)_2$ dimer and to a lesser extent compared to the more strongly bound complexes where HNC acts as a proton donor. However, these predicted shifts for all the complexes involving HNC, which up-to-date have not yet been experimentally characterized, should warrant their identification by their vibrational spectra. An important attempt to do this was the report by Evans and co-workers,[44] who studied iminoacetonitrile ($C_2H_2N_2$) in low-temperature argon matrixes. The decomposition process of the precursor gives $(HCN)_2$ dimers but also a set of new bands that the authors discussed to belong to some other species, possibly HNC complexes. Prominent bands of HNC were seen after 254 nm photolysis experiments, and two sets of bands were reported: 3330, 3298, 3237, 2125, 2077, 1350, 736, 706 cm^{-1}; 3240, 3166, 2115, 2058, 1024, 808 cm^{-1}. Both sets of bands originate from matrix isolated $C_2H_2N_2$ and might therefore belong to some HNC complexes. Indeed, most of these bands could be tentatively assigned by our calculated vibrational frequencies of the bimolecular complexes between HCN and HNC, but the experimental data presented are nevertheless inconclusive and consist of too many uncertainties. Therefore our ongoing investigation of formaldoxime photochemistry should shed light also on the problematics of the HCN and HNC bimolecular complexes.

Conclusions

The structures, vibrational spectra, and energetics of linear bimolecular complexes HNC···HNC, HCN···HNC, and HNC··· HCN were determined by ab initio methods. The hydrogen isocyanide dimer (HNC···HNC) was found to be the strongest complex, with an interaction energy of −28.6 kJ mol^{-1} at the CCSD(T)//MP3 level of theory (−29.5 kJ mol^{-1} at MP2). This interaction is much stronger than one found for HCN···HCN, being −17.9 kJ mol^{-1} (CCSD(T)//MP3) and −17.7 kJ mol^{-1} (MP2//MP2), respectively. The mixed HCN···HNC and HNC··· HCN complexes are of comparable proton donor strength with the monomolecular complexes. A comparison of CCSD(T), MP3, and MP2 optimized structures of HNC···HCN shows that the increased electron correlation does not significantly deform the complex structure, and the CCSD(T)//MP2 single-point calculations give resonably accurate interaction energies similar to a full CCSD(T) calculation at a much reduced computational cost.

An energy decomposition scheme based on the MP2 extended Morokuma analysis was carried out to study the various energy components involved in the intermolecular interaction. The largest contributions to the interaction energy come from the electrostatic and exchange interactions. The electron correlation terms do not increase the strength of the interaction for the HCN dimer, whereas the interaction energy originating from electron correlation is much greater for the HNC dimer. The mixed complexes HCN···HNC and HNC···HCN have significant contributions from both SCF and correlation levels. The decomposition analysis shows that the carbon−carbon hydrogen bond in the HNC···HCN complex has large energy contributions from both dispersion and exchange components, which indicates that the C···H−C bond is similar to conventional hydrogen bonds with N, O, or F as hydrogen acceptors and donors.

The calculated vibrational spectra of the complexes show large frequency shifts and intensity changes typical for strongly bound complexes. The comparison of MP2, MP3, and experimental results for $(HCN)_2$ indicates that MP3 frequency shifts are more accurate than MP2 shifts. The differences in the shifts of HCN and HNC vibrations for all of the complexes studied here parallel the computational and experimental results obtained for HCN−H_2O and HNC−H_2O.[19] Both experimental and ab initio HNC frequencies shift considerably more than their HCN counterparts, presumably due to larger perturbations of the electronic structure upon complexation, as the ab initio interaction energies of the two isomers do not vary as much as the frequency shifts.

Acknowledgment. The Academy of Finland and the Finnish Cultural Foundation are thanked for financial support to J.L. Prof. Latajka is acknowledged for interesting discussions during this work. The CSC-Center for Scientific Computing Ltd. (Espoo, Finland) is thanked for the mainframe time spent on the SGI Origin 2000 and Compaq AlphaServer SG140 computers during this study.

References and Notes

(1) Alkorta, I.; Rozas, I.; Elguero, J. *Chem. Soc. Rev.* **1998**, *27*, 163.
(2) Schleyer, P. v. R.; Allerhand, A. *J. Am. Chem. Soc.* **1962**, *84*, 1322.
(3) Ferstandig, L. *J. Am. Chem. Soc.* **1962**, *84*, 3553.
(4) Suzuki, S.; Green, P. G.; Bumgarner, R. E.; Dasgupta S.; Goddard, W. A., III; Blake, G. A. *Science* **1992**, *257*, 942.
(5) Rodham, D. A.; Suzuki, S.; Suenram, R. D.; Lovas, F. J.; Sagupta S.; Goddard, W. A., III; Blake, G. A. *Nature* **1993**, *362*, 735.
(6) Schleyer, P.,v. R.; Allerhand, A. *J. Am. Chem. Soc.* **1963**, *85*, 866.
(7) Schrems, O.; Huth, M.; Kollhoff, H.; Wittenbeck, R.; Knözinger, E. *Ber. Bunsen-Ges. Phys. Chem.* **1987**, *91*, 1, 1261 and references therein.
(8) Legon, A. C.; Millen, D. J.; Mjöberg, P. J. *Chem. Phys. Lett.* **1977**, *47*, 589.
(9) Ruoff, R. S.; Emilsson, T.; Chuang, C.; Klots, T. D.; Gutowsky, H. S. *Chem. Phys. Lett.* **1987**, *138*, 553.
(10) Jucks, K. W.; Miller, R. E. *J. Chem. Phys.* **1988**, *88*, 6059.
(11) Kerstel, E. R. Th.; Lehmann, K. K.; Gambogi, J. E.; Yang, X.; Scoles, G.; *J. Chem. Phys.* **1993**, *99*, 8559.
(12) Kofranek, M.; Lischka, H.; Karpfen, A. *Mol. Phys.* **1987**, *61*, 1519.
(13) King, B. F.; Weinhold, F. *J. Chem. Phys.* **1995**, *103*, 333.
(14) King, B. F.; Farrar, T. C.; Weinhold, F. *J. Chem. Phys.* **1995**, *103*, 348.
(15) Milligan, D. E.; Jacox, M. E. *J. Chem. Phys.* **1967**, *47*, 278.
(16) Maki, A. G.; Sams, R. L. *J. Chem. Phys.* **1981**, *75*, 4178.
(17) Pearson, P. K.; Schaefer, H. F. *J. Chem. Phys.* **1975**, *62*, 350.
(18) Alkorta, I.; Rozas, I.; Elguero, J. *Theor. Chem. Acc.* **1998**, *99*, 116.
(19) Heikkilä, A.; Pettersson, M.; Lundell, J.; Khriachtchev, L.; Räsänen, M. *J. Phys. Chem. A* **1999**, *103*, 2945.
(20) Frisch, M. J.; Trucks, G. W.; Schlegel, H. B.; Gill, P. M. W.; Johnson, B. G.; Robb, M. A.; Cheeseman, J. R.; Keith, T.; Petersson, G. A.; Montgomery, J. A.; Raghavachari, K.; Al-Laham, M. A.; Zakrzewski, V. G.; Ortiz, J. V.; Foresman, J. B.; Cioslowski, J.; Stefanov, B. B.; Nanayakkara, A.; Challacombe, M.; Peng, C. Y.; Ayala, P. Y.; Chen, W.; Wong, M. W.; Andres, J. L.; Replogle, E. S.; Gomperts, R.; Martin, R. L.; Fox, D. J.; Binkley, J. S.; Defrees, D. J.; Baker, J.; Stewart, J. P.; Head-Gordon, M.; Gonzalez, C.; Pople, J. A. *Gaussian 94*, revision E.2; Gaussian Inc.: Pittsburgh, PA, 1995.
(21) Frisch, M. J.; Trucks, G. W.; Schlegel, H. B.; Scuseria, G. E.; Robb, M. A.; Cheeseman, J. R.; Zakrzewski, V. G.; Montgomery, J. A., Jr.; Stratmann, R. E.; Burant, J. C.; Dapprich, S.; Millam, J. M.; Daniels, A. D.; Kudin, K. N.; Strain, M. C.; Farkas, O.; Tomasi, J.; Barone, V.; Cossi, M.; Cammi, R.; Mennucci, B.; Pomelli, C.; Adamo, C.; Clifford, S.; Ochterski, J.; Petersson, G. A.; Ayala, P. Y.; Cui, Q.; Morokuma, K.; Malick, D. K.; Rabuck, A. D.; Raghavachari, K.; Foresman, J. B.; Cioslowski, J.; Ortiz, J. V.; Baboul, A. G.; Stefanov, B. B.; Liu, G.; Liashenko, A.; Piskorz, P.; Komaromi, I.; Gomperts, R.; Martin, R. L.; Fox, D. J.; Keith, T. Al-Laham, M. A.; Peng, C. Y.; Nanayakkara, A.; Gonzalez, C.; Challacombe, M.; Gill, P. M. W.; Johnson, B.; Chen, W.; Wong, M. W.; Andres, J. L.; Gonzalez, C.; Head-Gordon, M.; Replogle, E. S.; Pople, J. A. *Gaussian 98*, Revision A.7; Gaussian, Inc., Pittsburgh, PA, 1998.
(22) Lundell, J. *J. Phys. Chem.* **1995**, *99*, 14290.
(23) Lundell, J.; Pehkonen, S.; Pettersson, M.; Räsänen, M. *Chem. Phys. Lett.* **1998**, *286*, 382.
(24) Boys, S. F.; Bernardi, F. *Mol. Phys.* **1970**, *19*, 553.
(25) (a) Morokuma, K. *J. Chem. Phys.* **1971,** *55*, 1236. (b) Kitaura, K.; Morokuma, K. *Int. J. Quantum Chem.* **1976**, *10*, 325.
(26) Latajka, Z. *J. Mol. Struct. (THEOCHEM)* **1991**, *251*, 245.
(27) Cybulski, S. M.; Couvillion, J.; Klos, J.; Chalasinski, G. *J. Chem. Phys.* **1999**, *110*, 1416.
(28) Chalasinski, G.; Szczesniak, M. M. *Mol. Phys.* **1988**, *63*, 205.
(29) Chalasinski, G.; Cybulski, S. M.; Szczesniak, M. M.; Scheiner, S. *J. Chem. Phys.* **1989**, *91*, 7048.
(30) Chalasinski, G.; Cybulski, S. M.; Szczesniak, M. M.; Scheiner, S. *J. Chem. Phys.* **1989**, *91*, 7809.
(31) Cybulski, S. M.; Chalasinski, G.; Moszynski, R. *J. Chem. Phys.* **1990**, *92*, 4357.
(32) Jeziorski, B.; van Hemert, M. *Mol. Phys.* **1976**, *31*, 713.
(33) Scheiner, S. *Hydrogen Bonding: A Theoretical Perspective*; Oxford University Press: New York, 1997; p 37 and references therein.
(34) See for example: Somasundram, K.; Amos, R. D.; Handy, N. C. *Theor. Chim. Acta* **1986**, *69*, 491.
(35) For a recent update of the C−H group involving in hydrogen bonding, see ref 33, p 298, and the following: Gu, Y.; Kar, T.; Scheiner, S. *J. Am. Chem. Soc.* **1999**, *121*, 9411.
(36) van Duijneveldt-van der Ridjt, J. G. C. M.; van Duijneveldt, F. B. In *Theoretical Treatments of Hydrogen Bonding*; Hadži, D., Ed.; Wiley: Chichester, U.K., 1997.
(37) van Duijneveldt, F. B.; van Duijneveldt-van der Ridjt, J. G. C. M.; van Lenthe, J. H. *Chem. Rev.* **1994**, *94*, 1873.
(38) At the MP2/6-311++G(2d,2p) level the dipole moments are 3.0198 and 3.2801 D for HCN and HNC, respectively, and at the MP3 level with the same basis set, the dipole moments are 3.0130 and 3.1157 D, respectively. The HCN dipole moment is virtually the same on both levels, indicating that the MP2 treatment of electron correlation in HCN is more complete than that of HNC.
(39) Hopkins, G. A.; Maroncelli, M.; Nibler, J. W.; Dyke, T. R. *Chem. Phys. Lett.* **1985**, *114*, 97.
(40) Wofford, B. A.; Bevan, J. W.; Olson, W. B.; Lafferty, W. J. *J. Chem. Phys.* **1986**, *85*, 105.
(41) Pacansky, J. *J. Phys. Chem.* **1977**, *81*, 2240.
(42) van Duijneveldt-van de Ridjt, J. G. C. M.; van Duijneveldt, F. B. *J. Comput. Chem.* **1992**, *12*, 399.
(43) Silvi, B.; Wieczorek, R.; Latajka, Z.; Alikhani, M. E.; Dkhissi, A.; Bouteiller, Y. *J. Chem. Phys.* **1999**, *111*, 6671.
(44) Evans, R. A.; Lorencak, P.; Ha, T.-K.; Wentrup, C. *J. Am. Chem. Soc.* **1991**, *113*, 7216.